# Calibration and Analysis of the GCT Camera for the Cherenkov Telescope Array

Jason J. Watson

Brasenose College
University of Oxford

*A thesis submitted for the degree of*
*Doctor of Philosophy*

Trinity 2018

## Abstract

Lorem ipsum dolor sit amet, consectetur adipiscing elit. Pellentesque sit amet nibh volutpat, scelerisque nibh a, vehicula neque. Integer placerat nulla massa, et vestibulum velit dignissim id. Ut eget nisi elementum, consectetur nibh in, condimentum velit. Quisque sodales dui ut tempus mattis. Duis malesuada arcu at ligula egestas egestas. Phasellus interdum odio at sapien fringilla scelerisque. Mauris sagittis eleifend sapien, sit amet laoreet felis mollis quis. Pellentesque dui ante, finibus eget blandit sit amet, tincidunt eu neque. Vivamus rutrum dapibus ligula, ut imperdiet lectus tincidunt ac. Pellentesque ac lorem sed diam egestas lobortis.

Suspendisse leo purus, efficitur mattis urna a, maximus molestie nisl. Aenean porta semper tortor a vestibulum. Suspendisse viverra facilisis lorem, non pretium erat lacinia a. Vestibulum tempus, quam vitae placerat porta, magna risus euismod purus, in viverra lorem dui at metus. Sed ac sollicitudin nunc. In maximus ipsum nunc, placerat maximus tortor gravida varius. Suspendisse pretium, lorem at porttitor rhoncus, nulla urna condimentum tortor, sed suscipit nisi metus ac risus.

Aenean sit amet enim quis lorem tristique commodo vitae ut lorem. Duis vel tincidunt lacus. Sed massa velit, lacinia sed posuere vitae, malesuada vel ante. Praesent a rhoncus leo. Etiam sed rutrum enim. Pellentesque lobortis elementum augue, at suscipit justo malesuada at. Lorem ipsum dolor sit amet, consectetur adipiscing elit. Praesent rhoncus convallis ex. Etiam commodo nunc ex, non consequat diam consectetur ut. Pellentesque vitae est nec enim interdum dapibus. Donec dapibus purus ipsum, eget tincidunt ex gravida eget. Donec luctus nisi eu fringilla mollis. Donec eget lobortis diam.

Suspendisse finibus placerat dolor. Etiam ornare elementum ex ut vehicula. Donec accumsan mattis erat. Quisque cursus fringilla diam, eget placerat neque bibendum eu. Ut faucibus dui vitae dolor porta, at elementum ipsum semper. Sed ultrices dui non arcu pellentesque placerat. Etiam posuere malesuada turpis, nec malesuada tellus malesuada.

# Calibration and Analysis of the GCT Camera for the Cherenkov Telescope Array


Jason J. Watson

Brasenose College

University of Oxford

A thesis submitted for the degree of

*Doctor of Philosophy*

Trinity 2018

# Acknowledgements


## Personal

Lorem ipsum dolor sit amet, consectetur adipiscing elit. Vestibulum feugiat et est at accumsan. Praesent sed elit mattis, congue mi sed, porta ipsum. In non ullamcorper lacus. Quisque volutpat tempus ligula ac ultricies. Nam sed erat feugiat, elementum dolor sed, elementum neque. Aliquam eu iaculis est, a sollicitudin augue. Cras id lorem vel purus posuere tempor. Proin tincidunt, sapien non dictum aliquam, ex odio ornare mauris, ultrices viverra nisi magna in lacus. Fusce aliquet molestie massa, ut fringilla purus rutrum consectetur. Nam non nunc tincidunt, rutrum dui sit amet, ornare nunc. Donec cursus tortor vel odio molestie dignissim. Vivamus id mi erat. Duis porttitor diam tempor rutrum porttitor. Lorem ipsum dolor sit amet, consectetur adipiscing elit. Sed condimentum venenatis consectetur. Lorem ipsum dolor sit amet, consectetur adipiscing elit.

Aenean sit amet lectus nec tellus viverra ultrices vitae commodo nunc. Mauris at maximus arcu. Aliquam varius congue orci et ultrices. In non ipsum vel est scelerisque efficitur in at augue. Nullam rhoncus orci velit. Duis ultricies accumsan feugiat. Etiam consectetur ornare velit et eleifend.

Suspendisse sed enim lacinia, pharetra neque ac, ultricies urna. Phasellus sit amet cursus purus. Quisque non odio libero. Etiam iaculis odio a ex volutpat, eget pulvinar augue mollis. Mauris nibh lorem, mollis quis semper quis, consequat nec metus. Etiam dolor mi, cursus a ipsum aliquam, eleifend venenatis ipsum. Maecenas tempus, nibh eget scelerisque feugiat, leo nibh lobortis diam, id laoreet purus dolor eu mauris. Pellentesque habitant morbi tristique senectus et netus et malesuada fames ac turpis egestas. Nulla eget tortor eu arcu sagittis euismod fermentum id neque. In sit amet justo ligula. Donec rutrum ex a aliquet egestas.

## Institutional

Lorem ipsum dolor sit amet, consectetur adipiscing elit. Ut luctus tempor ex at pretium. Sed varius, mauris at dapibus lobortis, elit purus tempor neque, facilisis sollicitudin felis nunc a urna. Morbi mattis ante non augue blandit pulvinar. Quisque nec euismod mauris. Nulla et tellus eu nibh auctor malesuada quis imperdiet quam. Sed eget tincidunt velit. Cras molestie sem ipsum, at faucibus quam mattis vel. Quisque vel placerat orci, id tempor urna. Vivamus mollis, neque in aliquam consequat, dui sem volutpat lorem, sit amet tempor ipsum felis eget ante. Integer lacinia nulla vitae felis vulputate, at tincidunt ligula maximus. Aenean

venenatis dolor ante, euismod ultrices nibh mollis ac. Ut malesuada aliquam urna, ac interdum magna malesuada posuere.

# Abstract

Lorem ipsum dolor sit amet, consectetur adipiscing elit. Pellentesque sit amet nibh volutpat, scelerisque nibh a, vehicula neque. Integer placerat nulla massa, et vestibulum velit dignissim id. Ut eget nisi elementum, consectetur nibh in, condimentum velit. Quisque sodales dui ut tempus mattis. Duis malesuada arcu at ligula egestas egestas. Phasellus interdum odio at sapien fringilla scelerisque. Mauris sagittis eleifend sapien, sit amet laoreet felis mollis quis. Pellentesque dui ante, finibus eget blandit sit amet, tincidunt eu neque. Vivamus rutrum dapibus ligula, ut imperdiet lectus tincidunt ac. Pellentesque ac lorem sed diam egestas lobortis.

Suspendisse leo purus, efficitur mattis urna a, maximus molestie nisl. Aenean porta semper tortor a vestibulum. Suspendisse viverra facilisis lorem, non pretium erat lacinia a. Vestibulum tempus, quam vitae placerat porta, magna risus euismod purus, in viverra lorem dui at metus. Sed ac sollicitudin nunc. In maximus ipsum nunc, placerat maximus tortor gravida varius. Suspendisse pretium, lorem at porttitor rhoncus, nulla urna condimentum tortor, sed suscipit nisi metus ac risus.

Aenean sit amet enim quis lorem tristique commodo vitae ut lorem. Duis vel tincidunt lacus. Sed massa velit, lacinia sed posuere vitae, malesuada vel ante. Praesent a rhoncus leo. Etiam sed rutrum enim. Pellentesque lobortis elementum augue, at suscipit justo malesuada at. Lorem ipsum dolor sit amet, consectetur adipiscing elit. Praesent rhoncus convallis ex. Etiam commodo nunc ex, non consequat diam consectetur ut. Pellentesque vitae est nec enim interdum dapibus. Donec dapibus purus ipsum, eget tincidunt ex gravida eget. Donec luctus nisi eu fringilla mollis. Donec eget lobortis diam.

Suspendisse finibus placerat dolor. Etiam ornare elementum ex ut vehicula. Donec accumsan mattis erat. Quisque cursus fringilla diam, eget placerat neque bibendum eu. Ut faucibus dui vitae dolor porta, at elementum ipsum semper. Sed ultrices dui non arcu pellentesque placerat. Etiam posuere malesuada turpis, nec malesuada tellus malesuada.

# Contents

# List of Figures

# Abbreviations

**AC** Alternating Current.

**ADC** Analogue-to-Digital Converter.

**ASIC** Application-Specific Integrated Circuit.

**CHEC** Compact High Energy Camera.

**CHEC-M** Compact High Energy Camera (CHEC) using Multi-Anode Photomultiplier Tubes (MAPMTs) as the detector.

**CHEC-S** CHEC using Silicon Photomultiplier Tubes (SiPMTs) as the detector.

**CTA** Cherenkov Telescope Array.

**DC** Direct Current.

**FEE** Front-End Electronics.

**FITS** Flexible Image Transport System.

**GCT** Gamma-ray Cherenkov Telescope.

**H.E.S.S.** High Energy Stereoscopic System.

**HV** High Voltage.

**IACT** Imaging Atmospheric Cherenkov Telescope.

**MAPMT** Multi-Anode Photomultiplier Tube.

**MST** Medium Size Telescope.

**NSB** Night-Sky Background.

**p.e.** Photo-Electrons.

**PDE** Photon Detection Efficiency.

**PMT** Photomultiplier Tube.

**RMSE** Root-Mean-Square Error.

**SiPMT** Silicon Photomultiplier Tube.

**SPE** Single Photo-Electron.

**TARGET** TeV Array Readout with GSa/s sampling and Event Trigger.

**TARGET 5** TARGET (TeV Array Readout with GSa/s sampling and Event Trigger) (version 5).

**TARGET C** TARGET (version C).

**Vped** Pedestal voltage input into the TARGET ASIC.

# 1

# Introduction

## Contents

:

# 1.1 Plan

## 1.1.1 Topics

- High Energy Astrophysics
  - Fermi
  - Fermi Bubbles
  - HAWC
- IACTs
- CTA
- CTA Science
  - Science Cases
  - Use "Science with CTA" paper
- SSTs
- SST Science
  - What do we contribute?
  - What can't be done without us?
- GCT
- CHEC
  - What makes us better?
  - Advantages of Schwarzchild-Couder
    - Increased FoV
    - Size
    - Cost
  - Advantages of full waveform readout
  - Other Advantages?
    - Trigger
    - Energy/power/voltage Requirements
    - Commonalities (SCT)

## 1.1.2 Questions

- ?

Shower properties, photons from bottom of shower are received before those at the top as the particle travels faster than light. Good figure in [1]

Gamma/Hadron/Lepton

# 2
# Camera Design & Mechanics

## Contents



:

## 2.1 Plan

### 2.1.1 Topics

- Introduce TARGET architecture & Wilkinson ADC
- Different TARGET versions
- FEE
- MAPMs
- SiPMS
  - How they work
  - Comparison investigations
  - Property trade-offs
- CHEC-M
- Changes for CHEC-S
- Future - MUSIC ASICs

### 2.1.2 Questions

- ?

## 2.2 Introduction

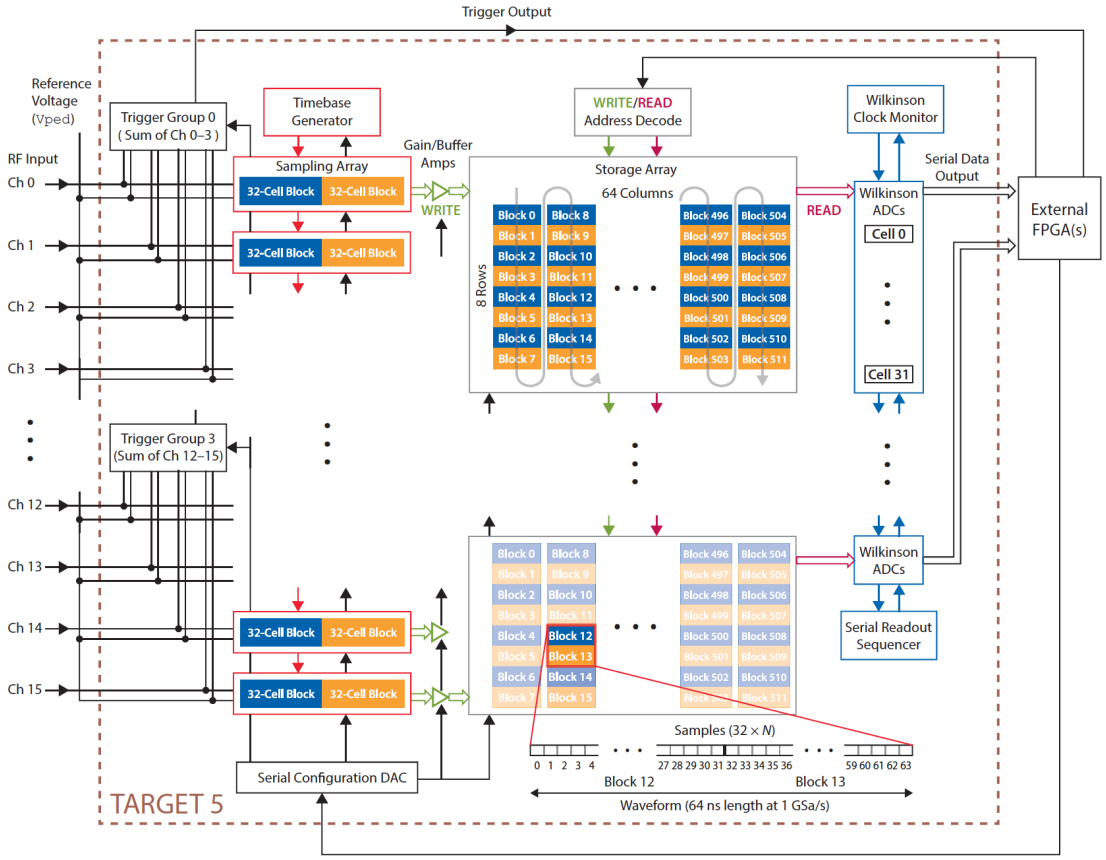


**Figure 2.1:** Functional block diagram of the TARGET 5 ASIC [2]

Add more details

# 3
# CTA Architecture

## Contents



:

## 3.1 Plan

### 3.1.1 Topics

- Requirements
- Data Levels

### 3.1.2 Questions

- ?

## 3.2 Introduction

## 3.3 Requirements

## 3.4 Data Levels

# 4 Software

## Contents



:

## 4.1 Plan

### 4.1.1 Topics

- TargetIO/TargetDriver
- TargetCalib
- ctapipe
- gammapy/CTOOLS

### 4.1.2 Questions

- ?

# 5

# Calibration

## Contents

:

## 5.1 Plan

### 5.1.1 Topics

- Pedestal subtraction
- Transfer functions
- Gain Matching
- SPE
- Flat fielding
- Time correction
- Future
  - Live calibration

### 5.1.2 Questions

- TARGET architecture diagram, Wilkinson ADC
- How much detail about all the TF approaches do I go into?

Flow diagrams? See Cyril talk 18/07/06 camera calibration call

## 5.2 Introduction

In order to obtain meaningful and reliable results from the camera, a number of calibrations must be applied to the waveforms read. A primary objective of my DPhil is to investigate the most optimal and efficient approaches for these calibrations (in accordance with the Cherenkov Telescope Array (CTA) requirements described in Chapter 3), and to determine if additional calibrations are required.

The calibrations applied have evolved during the course of the prototyping of CHEC; the calibrations applied to CHEC using MAPMTs as the detector (CHEC-M) waveforms are not the same for CHEC using SiPMTs as the detector (CHEC-S). Additionally, the calibration applied for the on-sky pipeline can differ slightly to the calibration used to obtain results such as the charge resolution.

When I joined the CHEC development, the calibration discussion was still in it's infancy. Some approaches had been tested in a laboratory environment [3], but there had been little discussion on how exactly the calibrations will be applied efficiently in an analysis pipeline, where one may not be able to use the same detailed calibration due to limited resources (such as memory and time). A major contribution of my DPhil was to prototype the calibrations procedures, develop an approach for a calibration pipeline, write the software to perform such a pipeline, and finally assess the performance of the pipeline. This was an iterative procedure,

the development of which is still ongoing, however a procedure now exists that allows us to obtain meaningful results from the waveform data, a capability that is of paramount importance in the commissioning of the camera.

In this chapter I will outline the each of the calibration steps that are presently adopted for CHEC camera. They are introduced in the general order that they are applied, and split into the categories of TARGET ASIC (Application-Specific Integrated Circuit), photosensor, and "other" calibrations.

## 5.3 TARGET Calibration

The calibrations described in this section relate to the TARGET module. As detailed in Chapter 2, the TARGET ASIC is responsible for the sampling, digitisation and readout of the waveform data. As a result there are two calibrations that are solely related to the TARGET ASIC: electronic pedestal subtraction and the linearity correction via the transfer function.

The functional block diagram of the TARGET ASIC in Figure 2.1 outlines the electronics responsible for the need of these calibrations, and should be used as a reference in the following descriptions.

As the calibrations in this section are very low-level, and related to CHEC's specific Front-End Electronics (FEE), they are handled by the TargetCalib library (described in Chapter 4).

### 5.3.1 Electronic Pedestal Subtraction

The most important, but also the simplest calibration to apply is the subtraction of the electronic pedestal. Each of the cells in the storage array of the ASIC is a unique capacitor. For a specific input input pedestal voltage (Vped), each capacitor has its own resulting electronic pedestal value. As each sample of the waveform corresponds to a single storage cell, each sample therefore has a unique pedestal value to be subtracted. This is apparent in Figure where the variation from sample-to-sample is very large. This variation is large enough that low amplitude pulses are undetectable in the waveform (Figure )) and therefore it is paramount to subtract this per-sample pedestal.

There are $2^{14} = 16,384$ storage cells per channel (for CHEC-M, $2^{12} = 4096$ for CHEC-S), therefore there are $32(Modules) * 64(Channels) * 16,384(Cells)$ pedestal values to keep record of. However, there is an additional contribution to the behaviour of the pedestal - discharging a cell to readout its value will slightly discharge adjacent cells. The result of this effect is that the further along in the

Create figure showing the raw waveform and its pedestal subtracted form (no HV)

Figure with low amplitude pulse before and after pedestal subtraction, and high amplitude pulse the same, also mirrored camera image?

Make sure to

**Figure 5.1**

Insert and update

waveform a cell is, the lower its pedestal value will be. An extra dimension of "position in waveform" consequently needs to be considered. This effect is illustrated in Figure , and its affect demonstrated in Figure .

include figures

### Generation

In order to perform the pedestal subtraction, one must first generate the lookup table of pedestal values. This can be easily obtained with a calibration run where the photosensors are disabled by turning off the High Voltage (HV) , and forcing the camera to trigger (with either an external pulse generator, or internally via software) to obtain a large amount of waveform data. Typically around 30,000 events provide enough samples for every storage cell, in every waveform position, to be hit at least 10 times. The samples are then collected as a running average with the dimensions $[Module, Channel, StartingBlock, Blockphase + Sample\_i]$, where the $StartingBlock$ is the storage block that the first sample in the waveform belongs to (see Figure ), $Blockphase$ is the cell index within the storage block that the waveform begins on, and $Sample\_i$ is the index of each sample in the waveform. This is illustrated in Figure , where for these two readout windows shown, the pedestal running average `Pedestal[TM][CHANNEL][9][8:103]` and `Pedestal[TM][CHANNEL][8][12:107]` will be contributed to respectively.

is it HV when considering the sipms?

include figure, and edit to use bp 8 and 12

Figure shows a visual representation of the pedestal lookup table for a single channel.

The TargetCalib library handles this generation, and stores the pedestal look-up table into a FITS (Flexible Image Transport System). A new pedestal file is typically generated at the start of each new dataset, as its dependencies on temperature and evolution with time are still being investigated.

A figure showing the lookup table of the pedestal, for checm due to the storage block ordering. Annotate a single repeated block

### Application

To apply the pedestal, the entry within the lookup table that corresponds to each sample is subtracted from the waveform. The result of the calibration can be seen in Figures .

talk about the variation in pedestal values, and mean? Talk bout the pattern seen between blocks

include figures from before

**Figure 5.2**

Insert and update, Also include extra plot versus event

### Performance

One quantification of this calibration's performance is the standard deviation per sample of the residual waveform from applying the pedestal subtraction to the data used to produce it. Figure 5.1 shows the spread in these values .

quote conversion into photo-electrons, and write actual resulting performance, and talk about if its good enough

This quantity informs about the intrinsic spread of the pedestal values about their mean, and can also indicate at some changes in pedestal value with time. Figure 5.2 demonstrates an occurrence of the pedestal value changing with time, and is investigated further in Section 5.5.2.

## 5.3.2 Transfer Function

The other calibration related to the digitisation and readout inside the TARGET ASIC is caused by the non-linearities in the storing and reading of charge to and from the storage cells. The components responsible for the need for this calibration are the sampling array, gain/buffer amps, and the Wilkinson Analogue-to-Digital Converters (ADCs), seen in Figure 2.1. As a result of the non-linearity of these components, the sample value readout does not scale linearly - a sample with twice the amplitude input into TARGET will have less than twice the amplitude when readout.

To correct for this non-linearity, a look-up table is generated to convert from the sample amplitude read-out (in ADC counts), to the input sample amplitude (in mV). This look-up table is known as the Transfer Function. As one might expect, each sampling cell has its own linear response to correct for, and therefore a look-up table is typically required at-least per channel and per sampling cell, however a noticeably improved performance is observed by considering a Transfer Function per storage cell .

need to show this, maybe in TF Investigations appendix?

There are two forms of Transfer Function that have been considered for CHEC, distinguished by the type of input used to generate them. A Direct Current (DC) Transfer Function is created by applying a constant DC input of known voltage into the module, and iterating over the full dynamic range by varying the voltage. An Alternating Current (AC) Transfer Function is generated by inputting an AC signal (such as a pulse with the expected shape from the photosensor plus shaper) of known amplitude, and iterating as with the DC approach. During previous investigations of the TARGET module, where sinusoidal signals were input into the module, a dependence on the signal frequency and input amplitude was observed that acts

to further reduce the output amplitude [3][2]. The source of this dependence was deemed to be due to the amplifiers, which cannot slew fast enough to keep up with the input signal if the frequency and amplitude are large.

### Generation (DC Transfer Function)

During the commissioning of CHEC-M, a DC Transfer Function was used with no AC corrections. To generate this Transfer Function the internal input pedestal voltage (Vped) setting is used to apply a DC voltage offset of known amplitude. The full dynamic range of the module is explored by repeating the process for amplitudes between . The waveforms produced by these runs are read-out, and the running average is grouped and monitored according to $[Module, Channel, SamplingCell, InputAmplitude]$, utilising every sample in the waveform. Around 1,000 events are required to provide sufficient statistics. This produces a lookup table like the one shown in Figure .

quote the range

insert figure

The second step in the generation is to flip the axes of this lookup table, and linearly interpolate at the ADC points defined by the user. This provides a second lookup table that can be more efficiently used to provide a calibrated mV value for the measured ADC value (Figure ). This table is saved to a FITS file, ready for application.

add figure

### Generation (AC Transfer Function)

As the ability to internally set a DC voltage with a known amplitude via the Vped was made more difficult in TARGET (version C) (TARGET C) (see 2) , and the ability to input a DC voltage externally is prohibited by the AC coupling of the module , the decision was made to transition to an AC Transfer Function that uses the expected pulse shape as an input. This approach therefore corrects for the AC effect with the appropriate frequency.

more precise ref, and remember to mention this change

remember to introduce ac coupling

The full dynamic range is once again explored, by injecting pulses of a variety of amplitudes. In order to extract the values that correspond to negative amplitudes in this method, the amplitude of the input undershoot is also monitored. Only the samples that corresponds to the maximum of the input pulse (and minimum of the undershoot) has a "true" amplitude of the input amplitude. Therefore to extract the correct samples, each waveform is fitted with two Landau functions, a fair approximation to the pulse shape (Figure ). Consequently, only two samples are extracted per waveform, requiring a much larger population of events ($\tilde{2}$00,000) in order to generate a reliable running average grouped according to $[Module, Channel, StorageCell, InputAmplitude]$. It is important to note that a

figure showing the fit

Transfer Function per storage cell was adopted for TARGET C, as it was found to significantly improve the residuals (see for further discussion).

appendix tf investigations

The second step in the generation is identical to the DC Transfer Function. The resulting lookup tables can be seen in Figures & .

add figures

### Application

Irrespective of the Transfer Function type, they are stored in a format which enables them to be applied identically. When calibrating a waveform, the relevant lookup table is obtained according to the channel and cell of the sample, and is linearly interpolated to provide the calibrated value in mV.

### Performance

Due to its complexity and variety of approaches, the Transfer Function is still one of the most actively discussed aspects of the CHEC calibration, and is most certainly the area where the majority of improvements can be made. Some possibilities for improvement include:

- An improved sample extraction method for the AC Transfer Function Waveform
- Possibilities for a DC approach for TARGET C
- Returning to the approach described in [2] where the pedestal is included inside the Transfer Function
- Alternatives to linear interpolation, such as Piecewise Cubic Hermite Interpolating Polynomial (PCHIP)
- Exchanging the lookup table for a parametrised regression characterisation of the Transfer Function
- Decision between "per storage cell" or "per sampling cell"
- Inclusion of temperature corrections

Appendix provides some insight into the current progression in these active investigations.

tf investigations

Assessing the performance of the Transfer Functions is a more complicated task than for the pedestals. This is largely because instead of a comparison to a null signal, you are instead comparing to an input amplitude which contains its own uncertainty,

and could potentially be incorrect. So while the residuals of the Transfer Function may be small, it does not necessarily mean the calibration is accurate. Therefore the most decisive performance indicator should be one that provides an independent measurement on the "correct" amplitude. The most obvious scheme fitting this requirement is the charge resolution, covered in detail by 7. However, while it does hold the drawbacks just mentioned, investigating the residuals through the Root-Mean-Square Error (RMSE) can provide insights on the Transfer Function calibrated unhindered by other components in the detector chain. Figure demonstrates the RMSE for the presently adopted Transfer Functions for TARGET C, compared to a simple calibration with a fixed conversion value $X$ $mv/ADC$ .

insert figure

obtain sensible value, and talk about the result a bit, non-linearity, show equation for RMSE

For ch7: Remember to talk about how the MC charge resolution provides us insight into performance with perfect Transfer Functions

## 5.4 Photosensor Calibration

The other primary component in the detector chain that requires calibration is the photosensor itself. As photosensors are a much more common instrument used in a variety of experiments, the calibration procedures typically already exist, and it is a simple case of adapting them to fit our needs.

However, unlike with the TARGET modules, where the procedures are very similar between CHEC-M and CHEC-S, an MAPMT is very different to a SiPMT. Therefore it is logical to deal with the calibration procedure for each of these photosensors separately.

### 5.4.1 CHEC-M

Photomultiplier tubes have been widely used in Gamma-ray Astronomy since the first Imaging Atmospheric Cherenkov Telescopes (IACTs) , therefore the characterisation of these devices is very well understood. However, MAPMTs are a more recent evolution of the devices, and although they have the same underlying concept, they do suffer from some limitations, such as the inability to tweak the HV on a pixel level, and the electrical crosstalk across the tightly packed pixels .

get source

check checm paper for other limitations

A common method to characterize MAPMTs, and the one we also adopted, is the use of the Single Photo-Electron (SPE) spectrum. The primary result this spectrum provides is the per pixel value to calibrate from the measured signal in mV (or mV*ns for integrated charge) to Photo-Electrons (p.e.). This conversion value is hereafter referred to as the SPE value. In order to investigate this parameter, the photosensor is illuminated with a very low light level (average illumination

<1 p.e. per pixel). As the photosensor is essentially a photon counting device, the individual peaks of the photoelectrons that are produced by the photocathode can be identified in the histogram of charge amplitudes. The SPE value is therefore the average charge of the first photoelectron peak. However, the resolution of these peaks can be quite poor, especially for MAPMTs, therefore the resulting distribution is fit with a function that characterises the photosensor:

add equation for mapm spe fit, and reference its origin

SPE fit plots

This SPE value is proportional to the gain of the photomultiplier, and therefore also proportional to the HV applied across the photomultiplier. In order to extract a clear SPE spectrum, the voltage across the MAPMTs are set to the maximum value of 1100 V, thereby maximising the separation between the photoelectron and pedestal peaks.

In order to extrapolate the correct SPE value for other HV settings, the following relation:

Can be used in combination with a logarithmic fit of a dataset where the amplitude is measured as a function of HV to obtain $\alpha$ per pixel.

double check, maybe linear regression in log space?

include plot of relation

plots of the SPE values at different hv sets

In order to apply this calibration, the SPE value (with units of $mV * ns * p.e.^{-1}$) per pixel is multiplied by the charge extracted per pixel.

show a waveform with this factor applied, maybe also the spectrum

### 5.4.2 CHEC-S

In the transition to SiPMTs, the calibration procedure for the photosensors was revised to better utilise the upgraded functionality of CHEC-S.

#### Gain Matching

Firstly, the voltage across the photosensors are now configurable per superpixel (group of 4 pixels) as opposed to per module. This allows the voltage to be fine-tuned to produce an identical gain response on a per superpixel level.

mention superpixels in ch3

The procedure for this is illustrated in Figure :

gain matching figure

- The camera is illuminated with approximately 50 p.e.
- The waveforms are readout and averaged per superpixel (excluding any dead pixels)

- The next voltage settings are calculated such that they will reduce the spread in the pulse height of the averaged waveforms

- The new voltage setting are applied, and the process is repeated

This iterating approach reduces the gain spread between pixels from (Figure ) values

need a note here or in ch2 about how other parameters of an sipmt change with hv

add final comparison figure

The additional benefit of this calibration is that changes in temperature, which would normally affect the gain, can be accounted for by changing the HV, therefore maintaining a constant gain response across the camera. This particular in situ calibration has not yet been implemented, but is intended for the future.

plot with gain vs temperature?

### SPE Calibration

The second step in the CHEC-S photosensor calibration differs according to the purpose of the dataset being calibrated. In order to completely characterise the camera, and produce the Charge Resolution results, the per pixel SPE value must be obtained, and used to produce the absolute charge in a waveform (the complete Charge Resolution procedure can be found in Chapter 8).

The function that characterises the SPE distribution of an SiPMT is not wildly different to that of an MAPMT, but does include the significant contribution of the optical crosstalk:

write function

The other significant difference in the SPE distribution of an SiPMT is the improved resolution of the peaks. Typically when an SiPMT is illuminated at , peaks from can be identified. Figure shows the SPE spectrum for the model of SiPMT we have installed into the camera. However, due to the inclusion of the other electronics in the camera, this incredible resolution is mostly suppressed, but is still significantly better than what was observed with CHEC-M. illumination

range of peaks

obtain spe figure of sipm on its own

Figure shows the SPE spectrum and fit for a pixel in our camera. The resulting parameters are reference chec-m figure

talk about the spe fit parameters, and show some histograms

insert figure

#### Flat-Fielding

Alternatively, in the default data-taking mode of on-sky Cherenkov images, the flat-fielding approach is used. This exists as a software extension to the gain-matching to further unify the response across the camera. With an illumination of approximately 50 p.e. (as with the gain matching), the coefficients are extracted such that the charge measured in each pixel is the same (after accounting for the difference in illumination between pixels due to the beam profile and curved geometry of the focal plane). These coefficients differ in those obtained via the SPE method as they include the relative Photon Detection Efficiency (PDE) between pixels in the correction.

The argument between flat-fielding according to gain response (SPE fitting) or according to illumination response (method we are adopting) is a common one among IACTs , and is also a current topic among the different CTA telescopes. The reason we have chosen to adopt the latter is it reduces the pixel-to-pixel variations in their response to being illuminated, which is important for Cherenkov shower images. The measured charge in each pixel will not be exactly representative of the number of photoelectrons, but instead it will be representative of the number of photons. However, in order to keep the charge extracted in relatable units, a single nominal $mV * ns * p.e.^{-1}$ conversion value will be applied to the entire camera.

find references where HESS/-MAGIC differ in their approach

needs some demonstration of its impact, some plots for example, that continue on from the gain matching plots

## 5.5 Other

In addition to the calibrations mentioned thus far, there are a few less important calibrations that could improve the performance further.

### 5.5.1 Timing Corrections

Due to the routing of the electronics in the front-end, the electrical signal path is slightly different per channel, causing a small difference in apparent arrival of the pulse in the waveform. The relative arrival time per pixel can be seen in Figure .

add camera image showing relative time

Not only does this need to be taken into consideration when investigating the timing performance, it also can have a significant impact on the charge extraction, which typically relies on other pixels (neighbouring or entire camera, see Chapter 6) sharing an compatible pulse time. The effect of a 1 ns incorrectly extracted charge (when the peak finding is done using the waveforms from all pixels) can have the impact on the charge resolution shown in Figure

show impact of an incorrect time extraction on charge resolution, maybe of just TM?

The first approach in correcting for this affect is to shift the charge extraction by the timing correction. However, current charge extraction methods do not operate

on time scales smaller than the waveform binning, therefore approaches on how to adapt those methods for corrections below that scale are being discussed.

### 5.5.2 Temperature Corrections

Temperature is most likely the most prominent factor in changing the calibration values on short scales, and has been mentioned in almost every approach. Investigations into exactly how these parameters change with temperature are ongoing, but examples can be seen in:

- Figure

  Pedestal ramp

- Figure

  TF Variation with temp

- Figure

  Gain variation with temp

In the future we intend to have a calibration pipeline that is independent of these temperature effects. For the photosensors this is very simple, as the voltage across them can be altered to account for the temperature changes. For the TARGET modules, this may require an additional lookup table, or an extra dimension to the existing tables.

### 5.5.3 LED Flashers

Although not technically a part of the waveform processing chain, the LED flashers have an important role in the calibration pipeline, especially for the final operation of the CHEC cameras in CTA. Their purpose is to allow us to perform in situ calibration, by uniformly illuminating the camera via reflection in the secondary mirror. However to achieve this, we must characterize and calibrate the LEDs such that we accurately know the illumination they are providing.

include some results on the LED calibration, and also mention their temperature dependence.

## 5.6 Future

During the long development of CHEC, the calibration procedure has evolved a lot, and multiple iterations have occurred to either:

- accommodate the changes required in the upgrades of hardware (such as from TARGET (version 5) (TARGET 5) to TARGET C)
- simplify the calibration to save on resources
- or account for additional factors, thereby improving the calibration (such as the AC contribution to the Transfer Functions)

Therefore, while each iteration improves in one aspect, it may be at the expense of the others. As a result, the TARGET calibration procedure described in this chapter appears quite complicated compared to the approaches detailed in [3] and [2]. The primary next step in the calibration development for CHEC is therefore to review the procedure used, with the aim to produce an approach that is simpler, includes aspects such as temperature dependence, and meets the requirements and processing rates required by CTA.

# 6

# Pipeline Reduction

## Contents

:

## 6.1 Plan

### 6.1.1 Topics

- Charge Extraction Methods
- Image cleaning
- Shower reconstruction
  - Hillas
  - Impact
  - model
  - Neural Nets
  - ++
- Energy Reconstruction
- Direction Reconstruction

### 6.1.2 Questions

- ?

## 6.2 Introduction

Following the low-level calibration detailed in 5, the waveforms should no longer require any further corrections unique to the electronics they were produced with. The waveforms from CHEC should now be in such a state that they can be processed in the same way as the waveforms from other cameras. This chapter describes the reduction performed on the waveforms in order to extract the Cherenkov shower information. With regards to the CTA data levels (Figure ), this concerns the steps from DL0 to DL2 .

figure with data levels in ch3

double check dl

These reduction methods have been a primary component of IACT analysis since the beginning of the field, therefore much thought and development has previously been performed on these techniques. As CTA is a large consortium that essentially consists of the worldwide IACT community, the developers of the reduction approaches for previous IACTs have brought them forward to CTA. However, due to:

(a) CTA is to consist of the most advanced IACTs to date, with higher shower imaging resolution and multiplicity than has previously been available

(b) the capabilities of digital signal processing has significantly increased in the past decade

The opportunity for more advanced and more successful algorithms exist within CTA. Some effort has already been made in this direction, but it is an aspect that is expected to constantly evolve and improve during the lifetime of CTA. In this chapter I will attempt to provide a broad overview of the existing and in-development reduction techniques, with an especial focus on charge extraction approaches due to my involvement in developing them.

improve sentence

## 6.3 Charge Extraction Methods

The most low-level reduction stage is the extraction of information from the calibrated waveforms provided by each camera individually. This procedure is very generic, allowing for the utilisation of common signal processing techniques that are not unique to Cherenkov shower analysis. The goal is to extract as much information from the pulse created by the Cherenkov shower light, while simultaneously limiting the amount of noise introduced from factors such as Night-Sky Background (NSB) . Two quantities are extracted in this stage: the signal charge in each pixel (the sums of which is a measure of the energy within the shower), and the signal arrival time per pixel.

talk about all the contributing factors (noise etc.) to waveforms in ch2

The total signal charge in a pixel, i.e. the total number of photo-electrons released from the Photomultiplier Tube (PMT)'s photocathode, is proportional to the total area below the pulse corresponding to the Cherenkov photons. If the waveforms were completely free of noise, and the readout window was large enough to capture the full Cherenkov signal, a simple integration of the entire readout would be a satisfactory approach for obtaining the signal charge. However, as we do not have the luxury of perfect waveforms, more complex methods are designed. Charge extraction algorithms typically consist of two aspects: how the signal pulse is found, and how the pulse is integrated.

### 6.3.1 Peak Finding

Two factors must be considered when finding the signal pulse of a Cherenkov shower. Firstly, the majority of camera pixels will not contain any Cherenkov signal while still containing noise. Secondly, due to the nature of Cherenkov showers (Chapter ), those pixels with Cherenkov signal will have different arrival times due to the time evolution of the Cherenkov image . This time gradient across the image is especially apparent for bright showers at a large core distance from the telescope. The most successful peak finding technique is the one that best accounts for those two factors. Some simple techniques used to define a peak time from a waveform include:

reference where the time gradient of Cherenkov showers are described

figure of peak time?

- **Local Peak Finding**: Each waveform is treated independently from the other. The maximum point in the waveform is treated as the peak/arrival time. This approach is intrinsically biased to assume every waveform contains a signal; therefore, in the absence of a Cherenkov signal, the largest noise pulse will be extracted, resulting in a higher total charge than should be obtained.

- **Global Peak Finding**: The waveform from every pixel is combined into an average, from which the maximum point is treated as the peak time for every pixel. This technique is only useful if a large portion of the camera is simultaneously illuminated, such as by a laser in the case of lab commissioning and calibration runs.

- **Neighbour Peak Finding**: The waveforms from the neighbouring pixels are combined into an average, from which the maximum point is treated as the peak time for the pixel-of-interest. This technique is often preferred for Cherenkov images as it has a reduced charge bias (especially if the pixel-of-interest's waveform is not included in the average); pixels with Cherenkov signal typically have neighbours that also contain Cherenkov signal at a correlated time, while the neighbours of empty pixels only contain noise, and therefore a random peak time is extracted.

- **Fixed Peak Value**: Due to a reliable definition of the camera trigger and subsequent electronic chain, the position of the pulse in the waveform could consistently be known a-priori, allowing for a fixed peak time. However, this method requires a larger integration window size in order to capture the full pulse in the tail of the Cherenkov shower, which occur at a later time than the initial photons which trigger the camera, therefore resulting in a larger noise included in the signal. However, this technique usually contains the least bias, as no signal is assumed to exist.

A more complex peak finding technique is the *Gradient Peak Finding* approach. This approach was designed for the VERITAS telescope [4][1][5], but is applicable to any IACT telescope with the ability of a dynamically choosing an integration window. *Gradient Peak Finding* is a two-pass approach where the time-gradient of the Cherenkov signal across the camera's focal plane is obtained by first extracting the signal using one of the other methods, and then cleaning and parameterising the image using simple techniques described later in this chapter. This time-gradient can then be used to assume a peak time based on camera pixel position. This

method provides a more unbiased estimation of the peak time of the signal at the expense of simplicity.

more verbose description from [1]

These peak finding methods have been described in relation to the maximum of the signal pulse, however they may instead use other characteristic positions of the pulse, such as the half-maximum time on the rising edge, or the centre of gravity of the pulse. Additionally, more advanced peak finding techniques may up-sample (possibly by zero-padding in the frequency domain via a Fourier transform) or interpolate the signal to obtain a more precise peak time [1][5], or even apply low-pass filters in order to remove low frequency baseline noise. The peak finding should be done in conjunction with any timing corrections () that may be required.

reference timing calibration section

maybe derive gradient here, and cross-correlation next, then each subsection has the full description of at least one complex algorithm

### 6.3.2 Integration

Once the peak time has been obtained, the simplest approach to extract the signal is to define an integration window centred about this time. The size of the window needs to be large enough to capture sufficient signal from the pulse, but small enough that not too much noise (NSB, dark counts, afterpulsing) is included within the window, thereby maximising the signal-to-noise. Additionally, the camera's pulse shape may not be symmetric, so a better signal-to-noise may be achieved by shifting the window a few samples with respect to the peak time. Typically, an integration window size on the order of ∼10 ns is used, with a shift of ∼3 ns. .

update values based on results

Beyond the simple "boxcar" integrator method (where every sample integrated has a weight of 1), other more advanced strategies may define their own alternative approach to extract the charge. One example is the fitting of the signal pulse, wither with an analytical description of the expected pulse, or with a more unconstrained description such as a cubic spline. A second complex approach is the use of digital filters, which can be used in combination with knowledge of the pulse shape to robustly extract the signal even in the presence of high noise. Such a technique has been designed and adopted for Gamma-ray Cherenkov Telescope (GCT), referred to as the *Cross-Correlation* method. Due to its adoption and sophistication, it is described here in more detail.

figures demonstrating the different peak finding

Cross-correlation is a common signal processing technique used as a measure of the similarity between two signals as a function of the displacement in time applied to one of the signals. Given a continuous function $f(t)$ defined between $0 \leq t \leq T$ and a second continuous function $g(t)$, the cross-correlation between the two functions $(f \star g)$ is defined as

$$(f \star g)(\tau) = \int_0^T \overline{f}(t) g(t+\tau) dt, \tag{6.3.2.1}$$

where $\overline{f}(t)$ is the complex conjugate of $f(t)$ and $\tau$ is the time displacement (also referred to as the "lag") between the two functions [6]. In descriptive terms, by varying $\tau$, $g(t+\tau)$ will slide past $f(t)$. The cross-correlation for a value of $\tau_1$ is then the integral across $t$ of the product between $f(t)$ and $g(t+\tau_1)$. For a discreet function that is real-valued, such as a sampled waveform, Equation 6.3.2.1 can instead be defined as

$$(f \star g)[n] = \sum_{m=0}^{N} f[m] g[m+n], \tag{6.3.2.2}$$

where $N$ is the total number of samples in the waveform and $m$ is the sample displacement.

An illustration of the *cross-correlation* approach being applied on a CHEC-S waveform is shown in Figure . The peaks in the cross-correlation result correspond to the displacements where the signals match best, and the values of the peaks correspond to an weighted integral of the entire waveform. Therefore, through utilising a template of the expected pulse shape in the absence of noise (hereafter referred to as the "reference pulse"):

figure showing the cross-correlation at a few different times, and the different stages, 3 axes, maybe for a low illumination? mention I implemented 6.3.2.2 in Python

- the individual pulses in the waveform are emphasised against other background contributions, improving the ability to find the signal pulse (using the same methods detailed in section 6.3.1)
- the charge contribution from the signal pulse is accentuated, while the noise contributions are diminished

The reference pulse we use for the cross-correlation is an obtained via probing the input analogue signal on the TARGET module and averaged on an oscilloscope. It is then normalised such that cross-correlation between it, and the reference pulse normalised to have an integral of 1, has a maximum value of 1. This normalisation ensures that the cross-correlation result is in units of $mV * ns$, and allows an easy conversion into $mV$ for "peak-height" investigations. An optimised implementation of cross-correlation exists in `scipy.ndimage.correlate1d` [7], where the waveforms for every pixel are processed in parallel.

### 6.3.3 Adopted approaches

Some examples of approaches adopted by other telescopes are outlined below.

### MAGIC

Members of the MAGIC telescope performed a study comparing the techniques proposed for their signal reconstruction. In [8] they compare four approaches: *fixed-window*, *sliding-window* with amplitude-weighted time, *cubic spline fit* with integral or amplitude extraction, and *digital filter*. It is concluded the digital filter, which relies on knowledge of the signal shape to minimise the noise contributions, provides a charge reconstruction with acceptable bias and minimal variance, while remaining stable in the occurrence of small variations in pulse shape and position.

### VERITAS

Similar to the aforementioned study for the MAGIC telescope, a comparison of charge extraction approaches was performed for VERITAS [4][1][5]. Specifically, the extraction methods compared include a *simple-window* using a-priori knowledge of the Cherenkov pulse time in the trace, a *dynamic-window* which slides across the trace to find the Cherenkov pulse, a *trace-fit* evaluator with fits the trace with two exponential functions which respectively describe the rise and fall time of the pulse, a *matched-filter* which "uses a digital filter based on the assumed shape of the FADC pulse to integrate the charge" [5], and finally an implementation of the "Gradient Peak Finding" approach described earlier in the chapter . At first glance, some of these approaches bear resemblance to those used by MAGIC, however there are slight differences:

should I move gradient peak finding to later, alongside the cross correlation method, as it has a nice analytical section from [1]

- in the VERITAS pulse fitting technique, an attempt to describe the pulse analytically was made whereas the MAGIC approach used a more loosely defined spline
- the filter used by VERITAS is a cross-correlation in Fourier space, whereas the filter used by MAGIC is generated using their knowledge of the noise auto-correlation matrix

Either as a result of these differences, or due to the difference in the instruments themselves, the *matched-filter* appears to result in a worse reconstruction than one would expect from the conclusion reached by MAGIC. One might justify that this degradation of signal extraction with the *matched-filter* for higher amplitudes is due to a change in pulse shape at higher amplitudes, thereby requiring a different "assumed FADC pulse shape", but it is not clear if that is what is occurring here. These studies conclude that the *matched-filter* "holds promise" for reconstructing low charges, whereas while the *trace-fit* performs extremely poor for the low charges (as expected), it performs the best for amplitudes $> 4$ photoelectrons [5].

#### H.E.S.S.

The standard mode of charge extraction for the High Energy Stereoscopic System (H.E.S.S.) telescopes is to integrate N samples with respect to a fixed, but regularly verified, signal time [9]. H.E.S.S. camera electronics underwent an upgrade in 2015/2016, subsequently allowing for the update of the standard extraction mode to also output time-of-maximum and time-over-threshold, and also allowed for full sample readout enabling the utilisation of more complex charge extraction techniques [10][11].

#### FlashCam

The FlashCam Medium Size Telescope (MST) proposed for CTA utilises a custom digital filter approach in which the 4 ns-spaced samples are up-sampled and deconvolved, resulting in an approximately Gaussian pulse with a 9 ns FWHM. In the linear (non-saturated) regime, the peak of this Gaussian is directly proportional to the signal charge. need reference

#### ASTRI

Contrary to the other techniques described in this section, ASTRI

### 6.3.4 Performance Assessment

Deciding on which charge extraction method to use is not trivial - as shown in the above discussion, different cameras may perform better with different algorithms. This is anticipated in *ctapipe* (4), where different `ChargeExtractor`s can easily be selected at runtime depending on the camera source.

## 6.4 Image Cleaning

### 6.4.1 Tailcut Cleaning

### 6.4.2 Wavelets

## 6.5 Shower Parameterisation

### 6.5.1 Hillas

### 6.5.2 Model and Model++

### 6.5.3 ImPACT

### 6.5.4 Neural Nets

## 6.6 $\gamma$-Hadron Separation

## 6.7 Energy Reconstruction

## 6.8 Direction Reconstruction

advanced techniques that don't fit into these categories, machine learning, photon counting

# 7

# Camera Performance

## Contents



:

## 7.1 Plan

### 7.1.1 Topics

- Charge Resolution
- TF Investigations
- Different NSB
- MC Validation
- MC Performance

### 7.1.2 Questions

- What other criteria?
  - Trigger performance - even though I haven't contributed

## 7.2 Introduction

## 7.3 Pulse Shape

## 7.4 Timing Characteristics

## 7.5 MC Validation

big diff between MC and the lab is the potential cross talk in the electronics and the effect e.g. of ground bounce - difference in full camera illumination

## 7.6 Charge Resolution

The most standard low-level criterion for performance used in CTA is the *Charge Resolution*. It encompasses both the bias and the standard deviation of the measured charge versus the expected charge to provide a measure of the waveform, calibration, and charge reconstruction quality. The CTA requirement

requirement label

(Chapter 3)

## 7.7 Conclusion

# 8
# On-Sky Pipeline

## Contents



:

## 8.1 Plan

### 8.1.1 Topics

- Decided upon reduction methods
- Potentially different than for performance chapter
- CHEC-M campaign
- MC CHEC-S
- Future observations
- Jupiter observations (Beyond cherenkov?)

### 8.1.2 Questions

- ?

# 9
# Summary

# Appendices

# A

# Transfer Function Investigations

## Contents



:

## A.1 Plan

### A.1.1 Topics

- AC vs DC
- Charge resolution of different approaches
- SPE spectrum

### A.1.2 Questions

- ?

# B

# Charge Extractor Investigations

## Contents



:

## B.1 Plan

### B.1.1 Topics

- RMS extracted charge with varying integration window size and shift with different NSBs and amplitudes (and combination of amplitudes)
- Charge resolution of different methods with different NSB (including full integration method)
- in the absence of the need for peak finding (laser illumination), and when peak finding is important (Cherenkov) - split into two, best integration technique (different NSBs, different integration window sizes), and best peak finding (different NSBs, need Cherenkov data)
- window size might actually change for Cherenkov - got to capture entire signal, and signal might not be centred at "calculated peak time".

### B.1.2 Questions

- ?

# References


[1] Peter Cogan and Sullivan Supervised by John Quinn. "Nanosecond Sampling of Atmospheric Cherenkov Radiation Applied to TeV Gamma-Ray Observations of Blazars with VERITAS". In: December (2006).

[2] A. Albert et al. "TARGET 5: A new multi-channel digitizer with triggering capabilities for gamma-ray atmospheric Cherenkov telescopes". In: *Astroparticle Physics* 92 (2017), pp. 49–61. URL: http://linkinghub.elsevier.com/retrieve/pii/S0927650517301524.

[3] K. Bechtol et al. "TARGET: A multi-channel digitizer chip for very-high-energy gamma-ray telescopes". In: *Astroparticle Physics* 36.1 (2012), pp. 156–165. URL: http://dx.doi.org/10.1016/j.astropartphys.2012.05.016.

[4] J. Holder and for the VERITAS Collaboration. "Exploiting VERITAS Timing Information". In: January (2005), pp. 383–386. URL: http://arxiv.org/abs/astro-ph/0507450.

[5] P Cogan and For The Veritas Collaboration. "Analysis of Flash ADC Data With VERITAS". In: *Methods* 0.1 (2007), p. 4. URL: http://arxiv.org/abs/0709.4208.

[6] Eric W. Weisstein. *"Cross-Correlation." From MathWorld–A Wolfram Web Resource.* [Online; accessed <today>]. URL: http://mathworld.wolfram.com/Cross-Correlation.html.

[7] *SciPy: Open source scientific tools for Python: scipy.ndimage.correlate1d.* [Online; accessed <today>]. URL: https://docs.scipy.org/doc/scipy/reference/generated/scipy.ndimage.correlate1d.html.

[8] J. Albert et al. "FADC signal reconstruction for the MAGIC telescope". In: *Nuclear Instruments and Methods in Physics Research, Section A: Accelerators, Spectrometers, Detectors and Associated Equipment* 594.3 (2008), pp. 407–419.

[9] F. Aharonian et al. "Calibration of cameras of the H.E.S.S. detector". In: *Astroparticle Physics* 22.2 (2004), pp. 109–125.

[10] S. Klepser et al. "Hardware and software architecture of the upgraded H.E.S.S. cameras". In: *Proceedings of Science* (2017), pp. 1–8.

[11] Raphaël Chalmé-Calvet et al. "Exploiting the time of arrival of Cherenkov photons at the 28 m H.E.S.S. telescope for background rejection: Methods and performance". In: *Proceedings of Science* 30-July-20 (2015).